On the radiation extinction of opposed flame spread over curved solid surface in low flow velocity conditions

Yusuke Konno[a]*, Nozomu Hashimoto[a], Osamu Fujita[a]*

[a]*Division of Mechanical and Space Engineering, Hokkaido University,*

Kita13, Nishi8, Kitaku, Sapporo, Hokkaido 060-8628, Japan

* Corresponding authors

E-mail address: y-konno@eng.hokudai.ac.jp (Yusuke Konno); ofujita@eng.hokudai.ac.jp (Osamu Fujita)

Tel: +81-11-706-6388 (Yusuke Konno); +81-11-706-6385 (Osamu Fujita)

Abstract

The controlling mechanisms of the radiation extinction of the flame spreading over cylinders in low flow velocity conditions are investigated with an analytical approach. Attention is focused on the interaction among solid surface curvature, solid surface radiation, and gas-phase volumetric radiation heat loss in the flame spread process. The analysis uses a classical thermal model, which considers the heat balance on the unburned fuel surface near the flame front. A non-dimensional number that evaluates the effects of volumetric radiation heat loss and finite rate chemistry on the flame temperature is also proposed. It is found that solid surface radiation cannot be a dominant mechanism for the radiation extinction of a flame spreading over a thin cylinder. Furthermore, in the case of flame spread over a cylinder, flame spread rate significantly increases with decreasing opposed flow velocity due to curvature effect, thus the consideration of the relative gas flow velocity seen by the spreading flame becomes essential in low flow velocity conditions. However, when the volumetric radiation heat loss in the gas phase is taken into account in the thermal model, flame spread rate for a thin cylinder once increases with decreasing opposed flow velocity and then turns to decrease. As a result, the flame spread rate of a thin cylinder shows a peak value in low flow velocity conditions. This trend is in good agreement with previous microgravity experiments (Fujita et al., 2002 [1]). Moreover, the limit condition of flame spread appears as a bifurcation point where the stable and unstable solutions of flame spread rate coincide in the low flow velocity condition. The analytical results indicate that it is essential to consider the volumetric radiation heat loss in the gas phase to predict the flame spread over a curved surface in low flow velocity conditions.

Keywords: Radiation extinction; Flame spread; Microgravity; Surface curvature, Radiation heat loss

Nomenclature

A	pre-factor
c_p	specific heat
d	diameter
Da	Damköhler number
E	activation energy
f_{cyl}	curvature factor
h	volumetric heat loss intensity
Δh_{c}	heat of combustion
H	heat loss parameter
L_{gx}	preheat heat zone
L_{gr}	standoff distance
L_{sr}	thermal penetration depth
$\dot{q}'''_{\mathrm{loss}}$	volumetric heat loss
r	radius
R	gas constant
Re	Reynolds number
T_{f}	flame temperature
T_{p}	pyrolysis temperature
$\boldsymbol{u}$	velocity vector
U	deviation of energy from equilibrium state
V_{f}	flame spread rate
V_{g}	gas velocity in mainstream
x_{d}	development length of boundary layer
X	mole fraction
Y	mass fraction

Greeks

α	thermal diffusivity
β	Zel'dovich number
γ	expansion ratio
δ_{f}	characteristic diffusion length in the flame
δ_{V}	velocity boundary layer thickness
ε	emissivity
κ_p	Plank mean absorption coefficient
λ	thermal conductivity
ν	kinematic viscosity
ρ	density
σ	Stefan-Boltzmann constant
τ	thickness
$\dot{\omega}'''$	reaction rate
Ω	correction factor of flame temperature
$\boldsymbol{\nabla}$	vector differential operator

Subscripts

eff	effective
F	fuel
g	gas
s	solid
st	stoichiometric
∞	ambient/initial

1. Introduction

The solid surface curvature is an important controlling factor that enhances the flame spreading over solid fuels [2]. Understanding the effect of solid surface geometries on the flame spread process is therefore not only important for fundamental combustion research but also essential for better fire safety design of materials. It has been well established that the preferential spread of flames along the edges and curved surfaces of solid fuels is due to the following reasons [1–5]: convex curvature on the flame surface facilitates access of oxygen to the flame and increases the ratio of the flame area to the solid surface, thereby enhancing the heat flux from the flame to the solid surface; the ratio of the surface radiation heat loss to the heat conduction from the gas phase to the solid surface becomes small compared to the flat surface thus flame spread is less affected by the surface radiation heat loss. It has been also reported in previous studies [1,3–5] that the effect of solid surface curvature on the flame spread process becomes more pronounced under low flow velocity conditions such as microgravity environment where there is no natural convection and therefore, molecular diffusion and radiation dominate the transport phenomena.

Flame spread over solid fuels in microgravity has been extensively studied with experiments, theoretical analysis, and numerical simulations, as reviewed by many researchers [6–11]. It is clarified that the radiation heat loss from the system suppresses the flame spread and leads to radiation extinction in microgravity. In addition, several previous studies [12–15] have shown that for flames spreading over solid fuels, unlike gaseous diffusion flame, solid surface radiation is the main mechanism of the radiation extinction rather than the volumetric heat loss in the gas phase.

Based on the above-mentioned considerations, previous studies [15–18] have developed thermal models [2], that take into account the heat balance at the surface of unburned fuel near the flame front, to describe the flame spread rate and extinction limit in microgravity conditions. For the slab, by considering the heat balance between the heat input from the flame to the solid surface and the radiation heat loss from the solid surface, quantitative predictions of the flame spread rate and radiation extinction in microgravity have been successfully achieved [15–18]. Although there have been several analyses [3,4,19] focusing on the effects of solid surface curvature and external gas flow velocity on the flame spread process, they studied only the steady flame spread problem. Thus, the effect of solid surface curvature on the extinction limits remains unclear. That is, the flame spread model over the curved solid surface is still in progress while the establishment of the flame spread model over the slab proceeds greatly. Moreover, in the existing analysis using thermal models, the effects of volumetric heat loss in the gas phase and finite rate chemistry are often ignored to simplify the analysis, and the adiabatic flame temperature is usually used for the analyses. This could be one of the challenges in the modeling of the flame spread over solid fuels.

Therefore, the present study aims to provide a more general model of the radiation extinction of flame spreading over a curved surface and then to provide a methodology estimating the flame spread rate and the radiation extinction limit in low flow velocity conditions. Particularly we consider the effects not only of the surface radiation heat loss but also of the volumetric radiation heat loss in the gas phase, which is a key process to estimate extinction limits. As an example of the flame spread over the curved solid surface, we study opposed flame spread over a thin cylindrical rod in which the curvature effect is pronounced.

2. Analysis

The energy balance equation for the opposed flame spread over a cylinder has been formulated by Delichatsios et al. [4]. Thus, the present analysis refers to their previous study [4]. The main change from the previous study is the incorporation of the effects of volumetric heat loss from the gas phase and finite rate chemistry on the flame temperature into the thermal model.

2.1. Energy balance equation

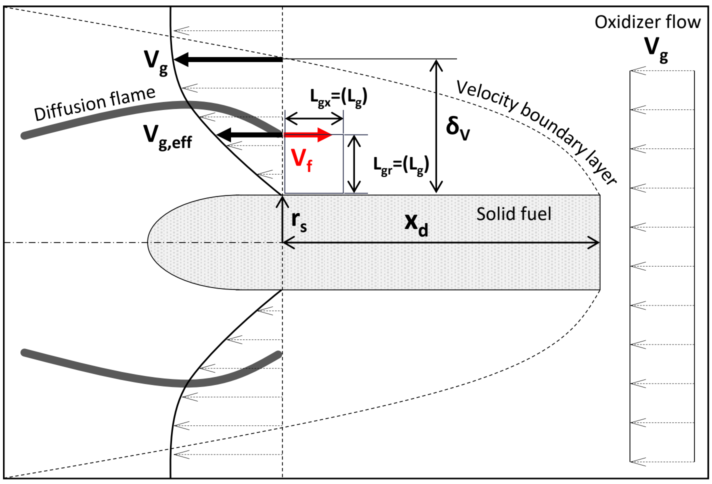

Figure 1: Schematic of opposed flame spread over a cylinder.

Figure 1 shows a conceptual diagram of opposed flame spread over a cylinder. A cylinder of radius r_s is placed in uniform flow with velocity V_g and diffusion flame enveloping a downstream edge of the cylinder travels with a constant velocity V_f in the opposite direction to the surrounding flow. A modified energy balance equation for the opposed flame spread over a cylinder is formulated as follows,

$$U(V_\mathrm{f}) = \Omega f_{\mathrm{cyl,g}} \lambda_\mathrm{g} (T_\mathrm{f} - T_\mathrm{p}) - L_\mathrm{g} \varepsilon_\mathrm{s} \sigma (T_\mathrm{p}^4 - T_\infty^4) - L_\mathrm{sr} f_{\mathrm{cyl,s}} \rho_\mathrm{s} c_{p,\mathrm{s}} V_\mathrm{f} (T_\mathrm{p} - T_\infty). \tag{1}$$

The LHS of Eq. (1) is the deviation of energy from the equilibrium state, which is a nonlinear function of V_f. Namely, V_f satisfying $U(V_\mathrm{f}) = 0$ corresponds to the steady solution of the spread rate. Note that for cylinder case Eq. (1) is a transcendental equation of V_f, and the solutions of V_f cannot be obtained analytically and must be obtained numerically. Moreover, since Eq. (1) in a nonlinear function of V_f, multiple steady solutions for V_f can be obtained; the typical behavior of $U(V_\mathrm{f})$ and the physical meaning of steady solutions are explained in Appendix A. The RHS of Eq. (1) consists of the heat conduction from the gas phase to the solid surface, the heat loss due to surface radiation, and the amount of energy required to heat the unburned fuel entering the control volume at a velocity V_f from ambient temperature, T_∞, to pyrolysis temperature, T_p. Although there are more sophisticated models that account for the heat of fusion and heat of gasification in the heat balance equation for steady flame spread problem [20,21], for the sake of brevity, the present analysis uses a simplified model that ignores melting and introduces a constant pyrolysis temperature, assuming that the activation energy of pyrolysis is sufficiently large. In Eq. (1), subscripts g and s denote gas and solid, respectively. In addition, Ω is the correction factor of the adiabatic flame temperature, f_cyl is the factor of the curvature, λ is the thermal conductivity, T_f is the flame temperature, T_p is the pyrolysis temperature of the solid fuel, L_g is the standoff distance (L_gr) or thermal diffusion length scale at the flame front (L_gx), ε is the emissivity, σ is the Stefan-Boltzmann constant, T_∞ is the ambient temperature, L_sr is the thermal penetration depth in the solid fuel from its surface, ρ is the density, and c_p is the specific heat.

L_g and L_sr are defined as follows [4,15,17],

$$L_\mathrm{g} = L_\mathrm{gx} = L_\mathrm{gr} = \alpha_\mathrm{g}/(V_\mathrm{g} + V_\mathrm{f}), \tag{2}$$

$$L_\mathrm{sr} = \min\left[r_\mathrm{s}, \sqrt{\alpha_\mathrm{s} L_\mathrm{g}/V_\mathrm{f}}\right], \tag{3}$$

where α is the thermal diffusivity. In the analysis, the relative gas flow velocity, $V_\mathrm{g} + V_\mathrm{f}$, to the spreading flame is introduced because the convection due to flame motion itself plays an important role in the flame spread process in low flow velocity conditions. In addition, to focus on the effect of the solid surface curvature on the flame spread, the present analysis is limited to the thermally thin case. Therefore, L_{sr} in Eq. (3) is calculated as $L_{\mathrm{sr}} = r_{\mathrm{s}}$ regardless of the solid fuel diameter. Another assumption introduced in the present analysis is that the longitudinal thermal length in the solid phase ($L_{\mathrm{sx}} = \alpha_{\mathrm{s}}/V_{\mathrm{f}}$) is considered to be L_{gx}, ignoring the heat conduction in the solid phase. This assumption is valid when $L_{\mathrm{gx}} > L_{\mathrm{sx}}$. Considering the thermophysical properties of plastic material used in the calculation (see Table 1), the assumption would be valid when V_{g} is less than 500 times of V_{f}, which is within the range of flow velocity condition in the present work. Therefore, it is reasonable to estimate the radiation heat loss from the solid surface by considering that L_{gx} is reflected on the solid surface in low flow velocity conditions. However, careful treatment of thermal length in the solid phase is necessary for high gas flow velocity conditions such as kinetic regime because L_{sx} can be larger than L_{gx}.

$f_{\mathrm{cyl,g}}$ and $f_{\mathrm{cyl,s}}$ are calculated as follows [4,19],

$$f_{\mathrm{cyl,g}} = \frac{CL_{\mathrm{g}}/r_{\mathrm{s}}}{\ln(1 + CL_{\mathrm{g}}/r_{\mathrm{s}})}, \tag{4}$$

$$f_{\mathrm{cyl,s}} = 1 - L_{\mathrm{sr}}/(2r_{\mathrm{s}}). \tag{5}$$

where C is a constant that modifies the heat flux from the flame to the solid surface [4]. In the present analysis, C is set to unity to simplify the discussion. It is noted that if r_{s} or V_{g} is sufficiently large, both $f_{\mathrm{cyl,g}}$ and $f_{\mathrm{cyl,s}}$ converge to unity (as $r_{\mathrm{s}} \to \infty$ or $V_{\mathrm{g}} \to \infty$, $f_{\mathrm{cyl,g}}$ tends to $0/0$ and therefore the limit of $f_{\mathrm{cyl,g}}$ may be evaluated by L'Hôpital's rule) and the curvature factors in both the gas phase and solid phase are eliminated. It is also noted that when $f_{\mathrm{cyl,g}}$ and $f_{\mathrm{cyl,s}}$ are set to unity, Eq. (1) is identical to the energy balance equation for the opposed flame spread over slabs. Based on properties of $f_{\mathrm{cyl,g}}$ and $f_{\mathrm{cyl,s}}$ with respect to V_{g}, the present study focuses on the radiation extinction under low flow velocity conditions.

Ω in Eq. (1) is a newly introduced dimensionless number in the present study. The role of Ω in the energy balance equation is the correction factor of the adiabatic flame temperature as discussed later to consider the effects of the volumetric heat loss and chemical reaction rate on the energy conservation in the gas phase which have been ignored in the conventional flame spread models over solid fuel surface. The details will be explained in a latter section.

2.2. *Effective gas flow velocity affecting the spreading flame*

Here, we modify gas flow velocity affecting the spreading flame by considering the development of the velocity boundary layer over the solid surface. Referring to the scale analysis developed by Bhattacharjee et al. [22,23], the gas velocity profile perpendicular to the solid surface ($V_{\mathrm{g}}(y)$) is defined, then the local gas flow velocity at the standoff distance of the flame leading edge ($y = L_{\mathrm{g}}$) is defined as $V_{\mathrm{g,eff}}$ (see Figure 1). In the present study, the Pohlhausen method [24] is adopted, then $V_{\mathrm{g}}(y)$ is calculated as follows,

$$V_{\mathrm{g}}(y) = \begin{cases} V_{\mathrm{g}}\left[\dfrac{3}{2}\left(\dfrac{y}{\delta_{\mathrm{V}}}\right) - \dfrac{1}{2}\left(\dfrac{y}{\delta_{\mathrm{V}}}\right)^3\right] & \text{for} \quad y < \delta_{\mathrm{V}} \\ V_{\mathrm{g}} & \text{for} \quad y \geq \delta_{\mathrm{V}} \end{cases}, \tag{6}$$

where $y = r - r_{\mathrm{s}}$, $\delta_{\mathrm{V}} = 4.64 x_{\mathrm{d}} Re_{x_{\mathrm{d}}}^{-0.5}$ is the thickness of the velocity boundary layer, x_{d} is the development length, $Re_{x_{\mathrm{d}}} = x_{\mathrm{d}} V_{\mathrm{g}} / \nu_{\mathrm{g}}$ is the Reynolds number, and ν is the kinematic viscosity. Substituting $y = L_{\mathrm{g}}$ in Eq. (6), $V_{\mathrm{g,eff}}$ is obtained as follows,

$$V_{\mathrm{g,eff}} = \begin{cases} V_{\mathrm{g}}\left[\dfrac{3}{2}\left(\dfrac{L_{\mathrm{g}}}{\delta_{\mathrm{V}}}\right) - \dfrac{1}{2}\left(\dfrac{L_{\mathrm{g}}}{\delta_{\mathrm{V}}}\right)^3\right] & \text{for} \quad L_{\mathrm{g}} < \delta_{\mathrm{V}} \\ V_{\mathrm{g}} & \text{for} \quad L_{\mathrm{g}} \geq \delta_{\mathrm{V}} \end{cases}. \tag{7}$$

$V_{\mathrm{g,eff}}$ in Eq. (7) will be used in the next section to define the non-dimensional quantities in the gas phase. It is important to note that since δ_{V} is a function of x_{d}, $V_{\mathrm{g,eff}}$ varies with the flame front position over the solid fuel. In fact, it has been confirmed experimentally [25,26] and numerically [27] that the opposed flame spread in the velocity boundary layer formed over the solid fuel surface shows unsteady behavior, and similarly the unsteady nature of flame spread can be discussed in the present model. However, since this study intends to discuss steady flame spread, x_{d} is fixed at 60 mm, and the eigenvalues of flame spread rate obtained in this case will be used for the discussion in the following sections.

2.3. *Correction factor of the adiabatic flame temperature*

To model the effects of the volumetric heat loss in the gas phase and finite rate chemistry on the flame temperature, we developed a non-dimensional number, Ω, based on the energy balance equation in the gas phase. The energy balance equation used in the analysis is as follows,

$$\rho_{\mathrm{g}} c_{p,\mathrm{g}} \boldsymbol{u} \cdot \boldsymbol{\nabla} T_{\mathrm{g}} = \lambda_{\mathrm{g}} \boldsymbol{\nabla}^2 T_{\mathrm{g}} + \Delta h_c \dot{\omega}''' - \dot{q}_{\mathrm{loss}}''', \quad (8)$$

where $\boldsymbol{u}$ is the velocity vector, $\boldsymbol{\nabla}$ is the vector differential operator, Δh_c is the heat of combustion per a unit mass of fuel, $\dot{\omega}'''$ is the reaction rate, $\dot{q}_{\mathrm{loss}}'''$ is the volumetric radiation heat loss. In the present study, the difference between mass and thermal diffusivity is not considered and the Lewis number is assumed to be unity.

The reaction rate follows the Arrhenius law as,

$$\dot{\omega}''' = \rho_{\mathrm{g}}^2 Y_{\mathrm{F}} Y_{\mathrm{O_2}} A e^{-E/(RT_{\mathrm{g}})}, \quad (9)$$

where Y_{F} is the mass fraction of the fuel, $Y_{\mathrm{O_2}}$ is the mass fraction of oxygen, A is the pre-factor, E is the activation energy, and R is the gas constant. For the simplicity of the analysis, the radiation heat loss is approximated as a linear function of gas temperature as [28–31],

$$\dot{q}_{\mathrm{loss}}''' = h(T_{\mathrm{g}} - T_\infty), \quad (10)$$

where h is the heat loss intensity and its unit is W/(m^3·K). Zhang et al. [30] and Chen [31] have confirmed that the linear and quartic radiative loss models have qualitatively and even quantitatively similar influences on the flame propagation of premixed gaseous fuels when the heat loss intensity is adjusted. Thus, in the present analysis, h in Eq. (10) is treated as an arbitrary constant and the contribution of the radiation heat loss in the gas phase to the flame spread and extinction will be investigated by changing the value of h. Note that, assuming that the gas is optically thin, h can be expressed as $h = 4\sigma\kappa_{\mathrm{p}} T_{\mathrm{f}}^3$ (where κ_{p} is the Plank mean absorption coefficient), so the calculation can be performed without making h as an arbitrary constant [28], but in this study h is treated as a constant to simplify the analysis and discussion.

To normalize Eq. (8), the characteristic diffusion length in the flame, $\delta_{\mathrm{f}} = \alpha_{\mathrm{g}}/(V_{\mathrm{g,eff}} + V_{\mathrm{f}})$, and the relative gas flow velocity seen by the flame, $V_{\mathrm{g,eff}} + V_{\mathrm{f}}$, are used as the reference length and velocity, respectively. The non-dimensional vectors are defined as,

$$\widetilde{\boldsymbol{\nabla}} = \delta_{\mathrm{f}}\boldsymbol{\nabla}, \qquad \widetilde{\boldsymbol{u}} = \boldsymbol{u}/(V_{\mathrm{g,eff}} + V_{\mathrm{f}}). \tag{11}$$

In addition, the non-dimensional quantities are defined as,

$$\tilde{T}_{\mathrm{g}} = (T_{\mathrm{g}} - T_{\infty})/(T_{\mathrm{f}} - T_{\infty}), \qquad \tilde{Y}_{\mathrm{F}} = Y_{\mathrm{F}}/Y_{\mathrm{F,st}}, \qquad \tilde{Y}_{\mathrm{O_2}} = Y_{\mathrm{O_2}}/Y_{\mathrm{O_2,\infty}}, \tag{12}$$

where $Y_{\mathrm{F,st}}$ is the mass fraction of fuel for stoichiometric combustion, $Y_{\mathrm{O_2,\infty}}$ is the mass fraction of oxygen in the oxidizer flow. The flame temperature can be calculated as,

$$T_{\mathrm{f}} = T_{\infty} + Y_{\mathrm{F,st}}\Delta h_{\mathrm{c}}/c_{p,\mathrm{g}} \tag{13}$$

The non-dimensional form for the energy balance equation in Eq. (8) is obtained as follows,

$$\widetilde{\boldsymbol{u}} \cdot \widetilde{\boldsymbol{\nabla}}\tilde{T}_{\mathrm{g}} = \widetilde{\boldsymbol{\nabla}}^2\tilde{T}_{\mathrm{g}} + Da\tilde{Y}_{\mathrm{F}}\tilde{Y}_{\mathrm{O_2}}e^{-\frac{\beta(1-\tilde{T}_{\mathrm{g}})}{1-\gamma(1-\tilde{T}_{\mathrm{g}})}} - H\tilde{T}_{\mathrm{g}}, \tag{14}$$

where Da is the Damköhler number, $\beta = \gamma E/(RT_{\mathrm{f}})$ is the Zel'dovich number, $\gamma = (T_{\mathrm{f}} - T_{\infty})/T_{\mathrm{f}}$ is the expansion ratio, H is the heat loss parameter. The relations of Da and H to the dimensional counterparts are as follows,

$$Da = \frac{\Delta h_c \rho_{\mathrm{g}}^2 Y_{\mathrm{F,st}} Y_{\mathrm{O_2,\infty}} A e^{-\beta/\gamma}}{\rho_{\mathrm{g}} c_{p,\mathrm{g}} (V_{\mathrm{g,eff}} + V_{\mathrm{f}})(T_{\mathrm{f}} - T_{\infty})/\delta_{\mathrm{f}}} = \frac{\alpha_{\mathrm{g}}\rho_{\mathrm{g}} Y_{\mathrm{O_2,\infty}} A e^{-\beta/\gamma}}{(V_{\mathrm{g,eff}} + V_{\mathrm{f}})^2}, \tag{15}$$

$$H = \frac{h(T_{\mathrm{f}} - T_{\infty})}{\lambda_{\mathrm{g}}(T_{\mathrm{f}} - T_{\infty})/\delta_{\mathrm{f}}^2} = \frac{h\lambda_{\mathrm{g}}}{\rho_{\mathrm{g}}^2 c_{p,\mathrm{g}}^2 (V_{\mathrm{g,eff}} + V_{\mathrm{f}})^2}. \tag{16}$$

Da in Eq. (15) stands for the ratio of the heat released by chemical reaction to the amount of energy required to heat the unburned gas entering the control volume at a velocity $V_{\mathrm{g,eff}} + V_{\mathrm{f}}$ from ambient temperature to the flame temperature. As seen in Eq. (15) Da decreases with increasing the gas flow velocity. This indicates that when the gas flow velocity is high the amount of heat released by the chemical reaction is depleted relative to the energy required to raise the temperature of the cold gas entering the reaction zone owing to the finite rate chemistry.

On the other hand, H in Eq. (16) stands for the ratio of the volumetric heat loss in the gas phase to the heat conduction in the gas phase. As seen in Eq. (16), H increases with decreasing the gas flow velocity. This implies that as the gas flow velocity decreases, the flame thickness increases, thus increasing the volumetric heat loss from the flame relative to the heat conduction from the flame to the surrounding or solid surface.

Considering the characteristics of Da and H derived from the energy balance equation in the gas phase, the linear combination of the inverse of Da and H well describes the extinction natures of the diffusion flame as a function of the flow residence time of the reactants. Therefore, we define a correction factor, Ω, of the adiabatic flame temperature as follows,

$$\Omega = 1 - 1/Da - H, \quad 0 \leq \Omega \leq 1. \tag{17}$$

$\Omega = 1$ corresponds to the assumptions of adiabatic flame ($H = 0$) and infinite rate chemistry ($Da = \infty$).

To better understand the characteristics of Ω, a simple calculation was performed here. Figure 2 shows the relationship between Ω and gas flow velocity and between the effective flame temperature, $T_{\mathrm{f,eff}}$ and gas flow velocity. $T_{\mathrm{f,eff}}$ is defined as follows,

$$T_{\mathrm{f,eff}} = T_{\infty} + \Omega(T_{\mathrm{f}} - T_{\infty}). \tag{18}$$

Namely, Ω can be considered as the dimensionless effective flame temperature. In the calculations, the adiabatic flame temperature of an air/C_2H_4 mixture with an equivalence ratio of unity is used. To see the effects of the chemical kinetic parameters and the volumetric heat loss on flame temperature, A is set to 3.0×10^7 $\mathrm{m^3/(kg \cdot s)}$ and β and h are varied. As can be seen in Figure 2, when both Da and H are considered in the calculation, Ω

and $T_{\mathrm{f,eff}}$ show upward convex trends with respect to the gas flow velocity. Moreover, as β increases, $T_{\mathrm{f,eff}}$ is more suppressed under high gas flow velocity conditions, while as h increases, $T_{\mathrm{f,eff}}$ is more suppressed under low velocity conditions. These trends correspond well with the relationship between the maximum flame temperature and the stretch rate for counterflow premixed flames [32] and between the maximum flame temperature and the gas flow velocity for counterflow diffusion flames [33], indicating that Ω is a useful dimensionless number for considering the effect of the flow residence time of the reactants on the flame temperature.

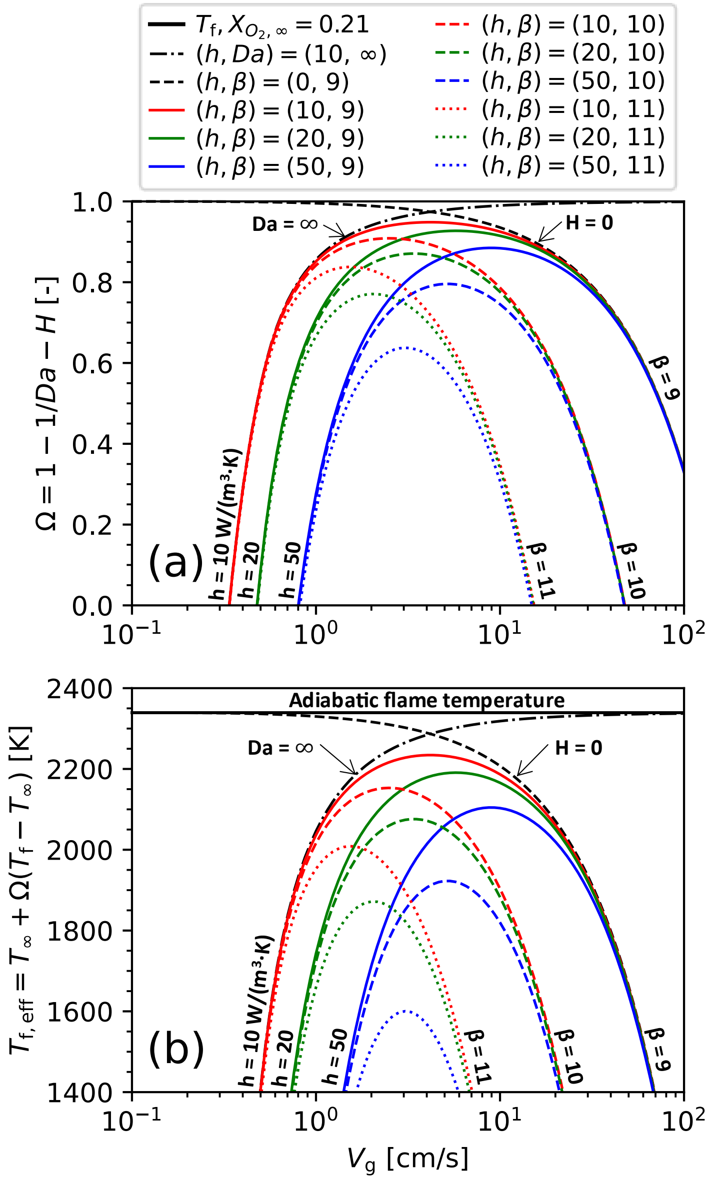

Figure 2: Relationship between Ω and gas flow velocity, (a) and between $T_{\mathrm{f,eff}}$ and gas flow velocity, (b).

3. Results and discussion

In this section, steady solutions of flame spread rate (V_f) that satisfies $U(V_f) = 0$ in Eq. (1) are presented. For the comparison, calculations are performed for both slab and cylinder. As mentioned before, when the calculation is performed for a slab, $f_{\mathrm{cyl,g}}$ and $f_{\mathrm{cyl,s}}$ in Eq. (1) are set to unity. Further, because the present study focuses on the effect of curvature on the radiation extinction in low flow velocity conditions, Da is purposely set to infinity in the analysis. Thus, Eq. (17) becomes $\Omega = 1 - H$. In the calculations, thermophysical properties of low-density polyethylene (LDPE) are used for solid fuel properties because comparable experiments using

LDPE coated electric wire in microgravity are available [1]. The thermophysical properties of LDPE used in the calculation are summarized in Table 1. A mixture gas of O_2 and N_2 is considered as the oxidizer. The flame temperature is calculated using NASA CEA2 [34].

Table 1: Properties of LDPE

Item	LDPE
Density, kg/m^3	920
Specific heat, J/(kg·K)	2300
Conductivity, W/(m·K)	0.33
Surface emissivity	1
Pyrolysis temperature, K	690

3.1. Without gas phase radiation ($H = 0$ and $Da = \infty$)

To confirm whether the surface radiation can extinguish a flame spreading over a cylinder in low flow velocity conditions or not, we firstly present the calculation results in which the heat loss from the system is only the surface radiation, ignoring the volumetric heat loss in the gas phase. For this purpose, Ω in Eq. (17) is set to unity.

V_f as a function of V_g for slab and cylinder are presented in Figure 3(a) and (b), respectively. To see the effect of solid surface curvature on V_f, the calculation results for four different fuel thicknesses/diameters (0.8, 2.0, 3.4, and 4.0 mm) are presented. For the slab (see Figure 3(a)), V_f decreases monotonically with decreasing V_g,

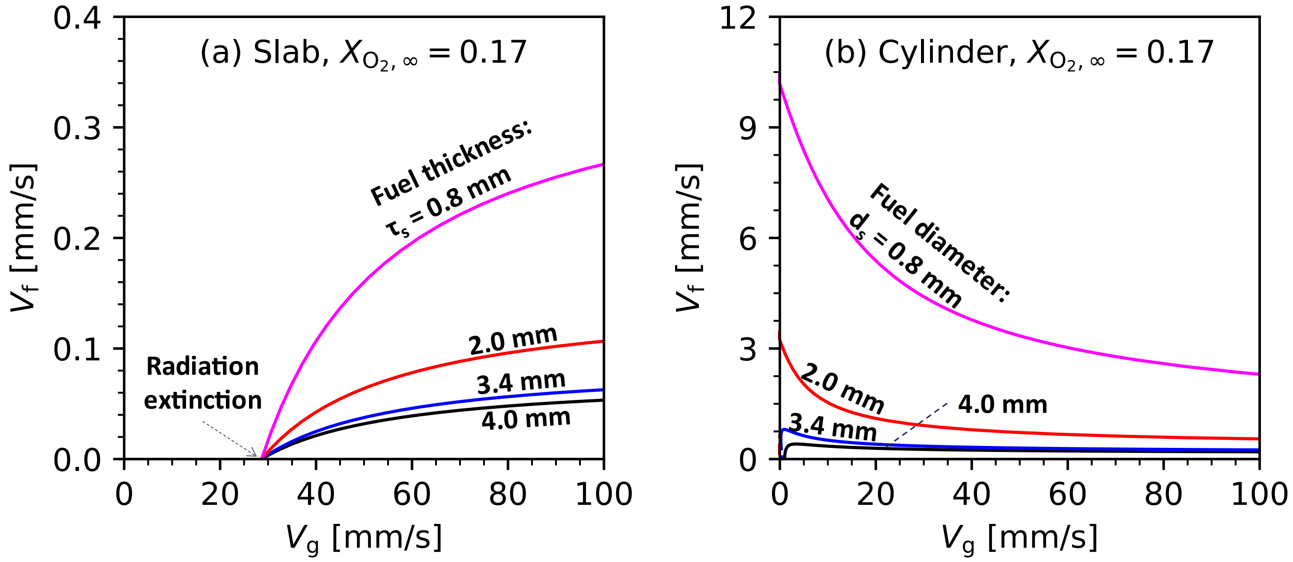

Figure 3: Flame spread rate, V_f, as a function of opposed flow velocity, V_g, at 17vol.% oxygen concentration with different fuel thickness. In the calculation. h in Eq. (16) is set to zero and the radiation heat loss in the gas phase is ignored. (a) is for slabs ($f_{cyl,g} = f_{cyl,s} = 1$) and (b) is for cylinders ($f_{cyl,g} \neq 1$ and $f_{cyl,s} \neq 1$).

and eventually V_{f} goes to zero irrespective of τ_{s}. Therefore, as reported by many researchers [12–16], we can understand the surface radiation plays a dominant role in the suppression of the flame spreading over slabs in low flow velocity conditions. Additionally, we can notice that although V_{f} increases with a decrease in τ_{s}, V_{g} at which V_{f} becomes zero does not change with τ_{s} within the range of the thickness calculated in the present analysis. Solving Eq. (1) for V_{g} satisfying $V_{\mathrm{f}} = 0$ yields,

$$V_{\mathrm{g,cr,slab}} = \frac{\varepsilon_{\mathrm{s}}\sigma}{\rho_{\mathrm{g}} c_{p,\mathrm{g}}} \frac{T_{\mathrm{p}}^4 - T_{\infty}^4}{T_{\mathrm{f}} - T_{\mathrm{p}}}. \tag{19}$$

Using Eq. (19), the gas flow velocity leading to radiation extinction can be easily estimated. As for the cylinder, $V_{\mathrm{g,cr,cyl}}$ is calculated as follows,

$$V_{\mathrm{g,cr,cyl}} = \frac{\alpha_{\mathrm{g}}/r_{\mathrm{s}}}{\exp[\alpha_{\mathrm{g}}/(r_{\mathrm{s}} V_{\mathrm{g,cr,slab}})] - 1}. \tag{20}$$

For the cylinder, the gas flow velocity leading to radiation extinction depends on the fuel radius because curvature plays an important role in the energy balance at the solid surface.

Moreover, for the cylinder (see Figure 3(b)), d_{s} has a significant effect on the qualitative trend of V_{f} with respect to V_{g}. For d_{s} = 4.0 mm, there is a velocity condition where V_{f} goes to zero, but when d_{s} is less than 2.0 mm, V_{f} increases monotonically as V_{g} decreases and exists as a positive real solution even at V_{g} = 0. It is noted that $V_{\mathrm{g,cr,cyl}}$ in Eq. (20) can always exist as a positive real number irrespective of r_{s}. The main cause of the unique behaviors of V_{f} with smaller d_{s} is that V_{f} itself can control the relative gas flow velocity seen by the spreading flame due to the increased V_{f}.

For further discussion, the results in Figure 3(b) are presented as log-log plots in Figure 4. In the figure, the condition where $V_{\mathrm{f}} = V_{\mathrm{g}}$ is denoted by the dotted diagonal line. We can notice that for smaller d_{s}, V_{f} becomes larger than V_{g} in low flow velocity conditions. It is also found that when V_{f} dominates the relative gas flow velocity seen by the spreading flame, the unstable solution of V_{f} appears as positive real solution (presented by dashed lines) and the unstable solution goes to zero at $V_{\mathrm{g,cr,cyl}}$ in Eq. (20) instead of the stable solution. It is noted that all calculation results presented in both Figure 3(a) and (b) have unstable solutions, but the ones that cannot be seen in the figures are negative quantities. The cause of the appearance of two flame spread rates under a certain condition is that Eq. (1) holds a negative feedback system, i.e., as V_f decreases, the heat loss from the system increases while enthalpy necessary for heating the unburned solid up to pyrolysis temperature decreases. Attention should be given that when the unstable solution exists as a positive real solution, Eqs. (19) and (20) cannot be used to estimate the limit condition of the flame spread because the gas flow velocity leading to radiation extinction will be overestimated when $V_f = 0$ is regarded as extinction.

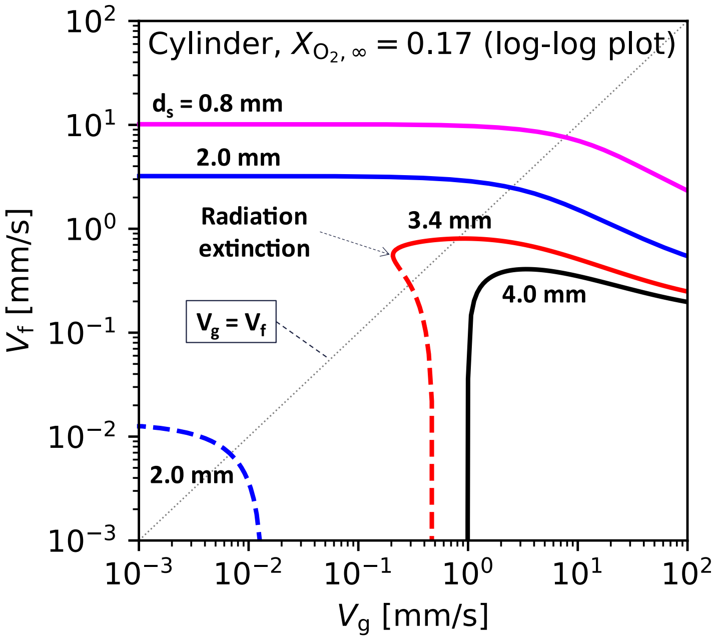

Figure 4: The calculation results in Figure 3(b) are presented as log-log plots. The solid and dotted lines correspond to the stable and unstable solutions, respectively. The dotted diagonal line corresponds to the condition where $V_g = V_f$.

From Figure 4, the following three types of solution behaviors can be identified depending on d_s:

(i) The stable solution goes to zero for $V_g \geq 0$ (when d_s is large, e.g., d_s = 4.0 mm).

(ii) The stable and unstable solutions become coincident at a positive real number for $V_g \geq 0$ (when d_s is transition range, e.g., d_s = 3.4 mm).

(iii) The stable and unstable solutions always exist as positive real numbers for $V_g \geq 0$ (when d_s is small, e.g., d_s = 2.0 and 0.8 mm (Unstable solutions exist outside the range of the graph)).

The solution behavior in type (ii) corresponds to the fold bifurcation [35] in the dynamical systems theory and the bifurcation point (quasi-stable solution) where the stable and unstable solutions coincide is also identified as the limit condition of the flame spread. This is also a characteristic solution behavior of systems with the negative feedback mechanisms.

The above results show that the radiation extinction of the flame spreading over solid fuels strongly depends on the solid surface curvature. Moreover, when the solid surface curvature is large enough, surface radiation cannot bring about the radiation extinction of the flame spreading over solid fuels. However, the monotonic increase in V_{f} with decreasing V_{g} for d_{s} = 2.0 and 0.8 mm is questionable. Fujita et al. [1] have experimentally investigated opposed flame spread over LDPE insulated nickel-chrome wire which has 0.5 mm core diameter and 0.65 mm or 0.8 mm outer diameter. Their experimental fact obtained in microgravity environment shows that V_{f} initially increases with decreasing V_{g}, then decreases when V_{g} approaches zero even with 21, 35, 50 vol.% oxygen concentrations [1]. Although the present analysis considers the flame spread over the fuel cylinder, comparison with experimental data from previous studies suggests that the thermal model which ignores the volumetric radiation heat loss in the gas phase cannot reproduce the actual flame spread phenomenon over a cylinder in microgravity conditions. In the next section, we, therefore, present calculation results that include the volumetric radiation heat loss in the gas phase to see the applicability of the model proposed in this study.

3.2. With gas phase radiation ($H \neq 0$ and $Da = \infty$)

As mentioned before, the contribution of radiation heat loss in the gas phase to the flame spread over solid fuels is modeled by treating h in Eq. (16) as a variable. In the present analysis, h was varied in the range of 0 – 50 W/(m^3·K), where the qualitative trend of V_{f} as a function of V_{g} varied significantly. Figure 5(a) and (b) show V_{f} as a function of V_{g} that include the effect of radiation heat loss in the gas phase. As in the previous section, the results for both the slab and cylinder are presented for comparison. Oxygen concentration and fuel thickness/diameter are fixed at 21vol.% and 0.8 mm, respectively.

For the slab (Figure 5(a)), as h increases, V_{f} decreases and the gas flow velocity leading to the radiation extinction ($V_{\mathrm{f}} = 0$) increases. As discussed before, the trends of V_{f} with respect to V_{g} for the slab is dominated by the surface radiation heat loss, thus the introduction of the radiation heat loss in the gas phase results in only

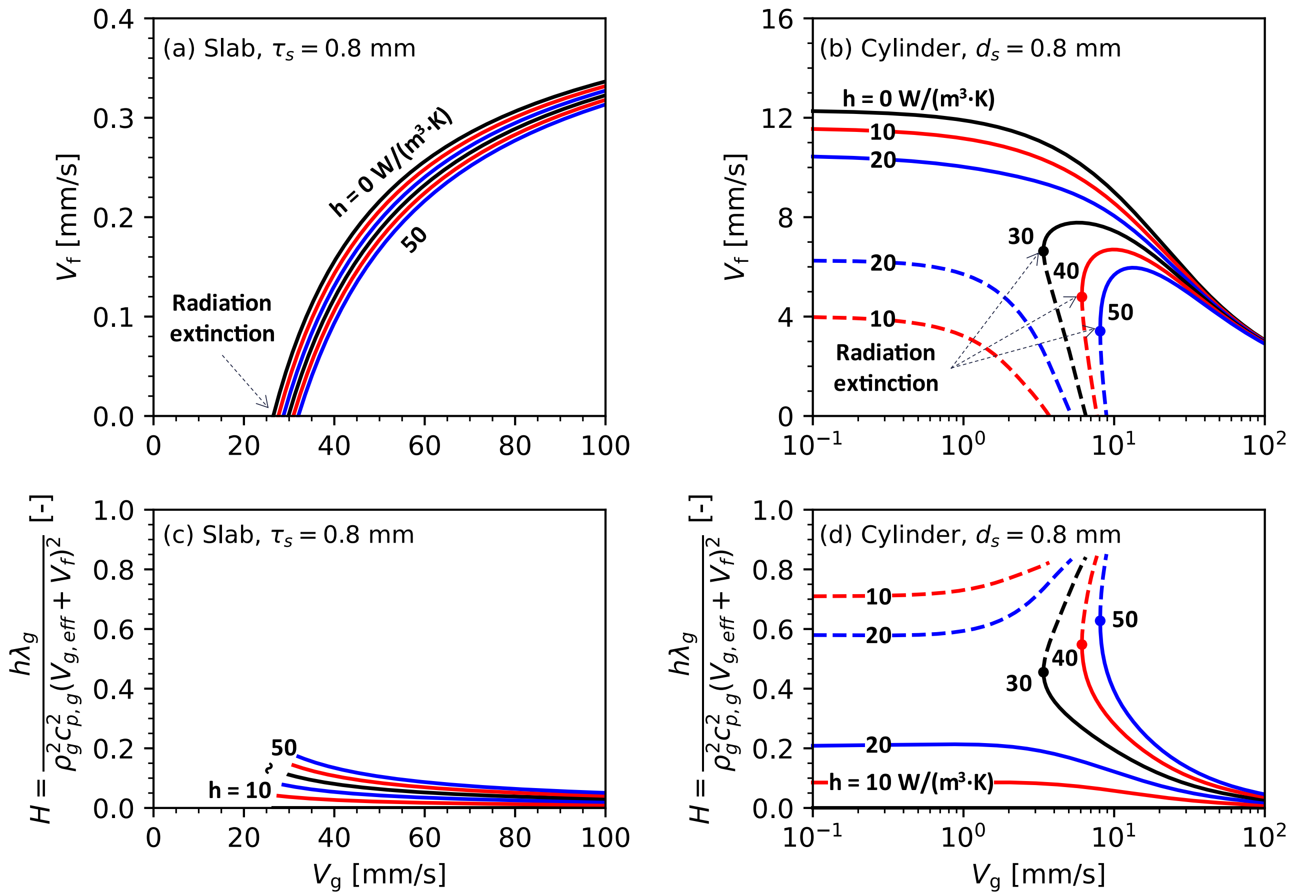

Figure 5: V_f and H as a function of V_g at 21vol.% oxygen concentration with different volumetric heat loss intensity, h. (a) and (c) are for a slab with 0.8 mm thickness and (b) and (d) are for a cylinder with 0.8 mm diameter.

a slight change in the quantitative results.

On the other hand, for the cylinder (Figure 5(b)), the qualitative trend of V_f with respect to V_g is affected significantly depending on the magnitude of radiation heat loss in the gas phase. As h increases, the stable solutions on the upper side decrease while the unstable ones on the lower side increase. In the figure, when h exceeds 30 W/(m^3·K), the stable solution once increases with decreasing V_g and then decreases. This trend is in good agreement with previous experimental results that investigated flame spread over a thin electric wire in microgravity low flow velocity conditions [1]. In addition, the appearance of the bifurcation point is confirmed in low flow velocity conditions indicating the radiation extinction. For further validation, a comparison of the experimental data for V_f of the wire sample with the calculated V_f of the cylinder is shown in Appendix B. Figure

B1 shows that by considering heat losses in the gas phase, it is possible to reproduce the experimentally observed non-monotonic trend of V_{f} with respect to V_{g}.

In Figure 5(c) and (d), H is also shown as a function of V_{g} to clarify the control mechanism of extinction of the flame spreading over the slab and cylinder. It is noted that H in Eq. (16) represents the ratio of radiation heat loss to the heat conducted from the flame to the surroundings. As can be seen in Figure 5(c) and (d), H increases with decreasing V_{g} and increasing h for both slab and cylinder cases. However, it can be seen that flame spreading over the slab is extinguished for $H < 0.2$, whereas that over the cylinder is extinguished for $H > 0.4$. From those results, it is demonstrated that the volumetric heat loss in the gas phase plays a significant role in the flame spread over a cylinder in low flow velocity conditions. Namely, the radiation extinction over an appreciably curved surface is dominated by the volumetric heat loss in the gas phase rather than the surface radiation heat loss.

Finally, we would like to mention the limitations of this model and future work. In this study, we demonstrated that a method to evaluate the dependence of flame temperature on ambient flow velocity via one-dimensional approach is effective. Furthermore, it was shown that heat loss in the gas phase plays a dominant role in flame spread and extinction when curvature exist on the solid surface. However, the validation of this model remains a qualitative discussion, and further optimization of input parameters such as h and reaction parameters (A and E) in Ω should be conducted through comparison with experimental results and numerical analysis. Note that long-term microgravity experiments are required to observe radiation extinction under low flow velocity conditions, and a detail comparison with experiments on orbit will make the discussion more quantitative. Additionally, the flame temperature should depend on the three-dimensional geometry of the gas phase, soot formation, heat of pyrolysis, and rate of pyrolysis of solid materials. The present model does not include those effects and it is limited up to qualitative estimation of flame spread rate. The sensitivity analyses of individual process should be made in numerical approach in the next step, while the main contribution of the present work is to show the necessity to consider gas phase radiative heat loss to reproduce the decrease trend in flame spread rate over curved surface solid in very low flow velocity conditions.

4. Conclusions

A theory of opposed flame spread and radiation extinction over a cylinder is developed based on a classical thermal theory. In the analysis, the effects of solid surface curvature, surface radiation heat loss, volumetric heat loss in the gas phase on the flame spread rate and extinction limit are assessed. It was found that surface radiation cannot be a mechanism for the suppression of the flame spread over solid fuel when the surface curvature is large. It was also found that the conventional theory cannot predict radiation extinction because the flame spread rate increases monotonically with decreasing gas flow velocity, even for a cylinder with a diameter of 2 mm under oxygen concentration of 17vol.%. When the flame spread rate increases significantly under low flow velocity conditions, the relative gas flow velocity seen by the spreading flame is dominated by the spread rate itself, and consequently, radiation extinction does not occur even in a quiescent environment. In addition, when the spread rate itself controls the relative gas flow velocity, the negative feedback mechanism in the system becomes apparent. As a result, extinction limits appear as the fold bifurcation point. When a non-dimensional number, Ω, which compensates the adiabatic flame temperature for the volumetric heat loss in the gas phase, is newly introduced into the thermal model, the model successfully reproduces the decrease in the spread rate and radiation extinction under low flow velocity conditions even with large solid surface curvature. It was confirmed that the trend of V_{f} calculated by the proposed model well reproduced the previous microgravity experimental results [1].

Acknowledgments

This research was supported by JAXA as a candidate experiment for the third stage use of JEM/ISS titled “Evaluation of gravity impact on combustion phenomenon of solid material toward higher fire safety” (called “FLARE”). This research was also supported by JSPS KAKENHI grant numbers JP19J10187 and JP21K20389.

Appendix A. Existence of two flame spread rates

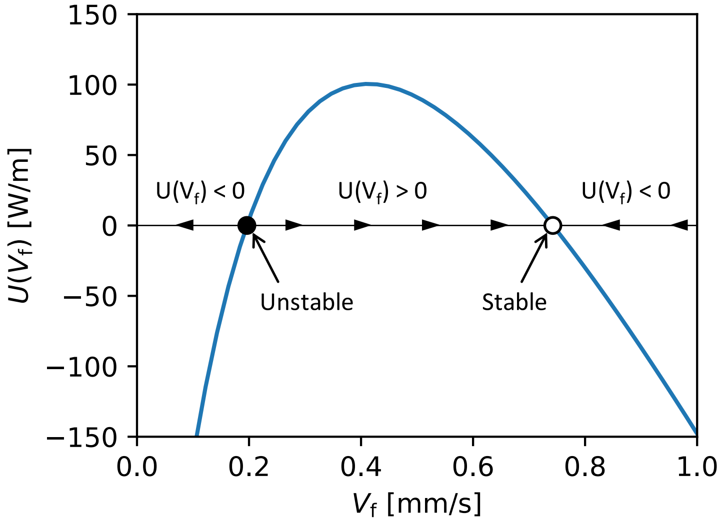

Figure A1: Mapping of $U(V_\mathrm{f})$ in Eq. (1) for a cylinder with $d_\mathrm{s} =$ 3.4 mm at $V_\mathrm{g} =$ 0.35 mm/s, 17vol.% oxygen concentration, and $\Omega = 1$.

The trend of $U(V_\mathrm{f})$ in Eq. (1) under the condition where the two flame spread rates are obtained as positive real solutions is shown in Figure A1. As can be seen in the figure, $U(V_\mathrm{f})$ shows an upward convex parabolic-like trend. This is because as V_f decreases, the enthalpy required for flame spread decreases, but at the same time heat loss increases. Additionally, because $U(V_\mathrm{f})$ is the deviation of energy from the equilibrium state, the stability of the solution can be discussed qualitatively by looking at the sign of $U(V_\mathrm{f})$ in the vicinity of the steady solutions. When $U(V_\mathrm{f}) > 0$, i.e., the energy balance in the entire system is in a surplus state, V_f should increase and vice versa. In other words, $U(V_\mathrm{f})$ can be regarded as the time derivative of V_f ($\mathrm{d}V_\mathrm{f}/\mathrm{d}t$). Therefore, as represented by the arrows in Figure A1, the flow of V_f is to the right where $U(V_\mathrm{f}) > 0$ and to the left where $U(V_\mathrm{f}) < 0$. At the points where $U(V_\mathrm{f}) = 0$, there is no flow, and they represent the steady solutions of V_f. Based on the vector diagram shown in Figure A1, the larger solution can be considered as a stable solution and the smaller solution as an unstable solution.

Appendix B. Comparison of experimental and calculated results

Figure B1 compares the experimental values of V_f obtained in the previous study by Fujita et al. with V_f calculated from the model developed in this study. Note that in the previous study, LDPE insulated NiCr wire with an outer diameter of 0.8 mm and a core diameter of 0.5 mm was used as the experimental sample, whereas in the present study, the calculations were performed on LDPE rods with an outer diameter of 0.8 mm. As shown in Figure B1 the conventional model, which ignores heat losses in the gas phase, cannot reproduce the experimental results at all under low flow velocity conditions because V_f increases monotonically as V_g decreases. However, by taking into account the heat losses in the gas phase, the V_f shows a non-monotonic trend with respect to V_g, as observed in the experiment, making it possible to predict a decrease in V_f and radiation extinction under low flow velocity conditions.

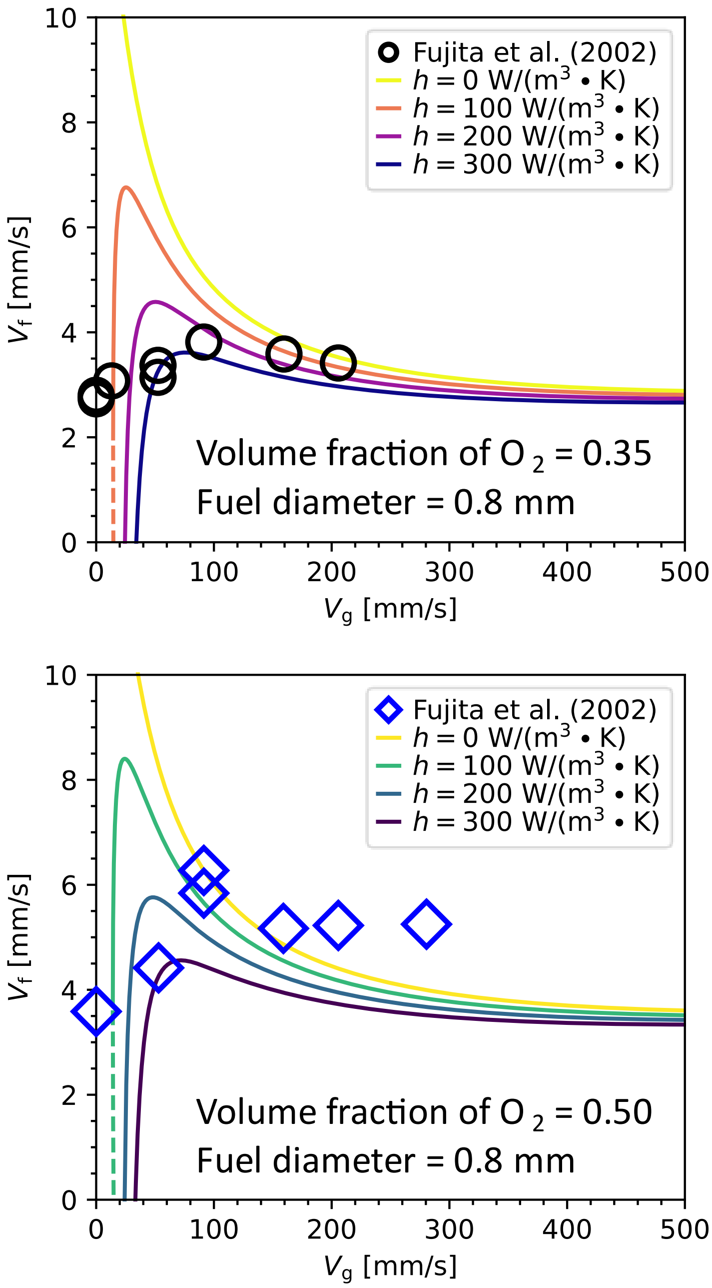

Figure B1: Flame spread rate as a function of opposed flow velocity.

References

[1] O. Fujita, K. Nishizawa, K. Ito, Effect of low external flow on flame spread over polyethylene-insulated wire in microgravity, Proc. Combust. Inst. 29 (2002) 2545–2552.

[2] F.A. Williams, Mechanisms of fire spread, Symp. Combust. 16 (1977) 1281–1294.

[3] F.J. Higuera, A. Liñán, Flame spread along a fuel rod in the absence of gravity, Combust. Theory Model. 3 (1999) 259–265.

[4] M.A. Delichatsios, R.A. Altenkirch, M.F. Bundy, S. Bhattacharjee, L. Tang, K. Sacksteder, Creeping flame spread along fuel cylinders in forced and natural flows and microgravity, Proc. Combust. Inst. 28 (2000) 2835–2842.

[5] O. Fujita, M. Kikuchi, K. Ito, K. Nishizawa, Effective mechanisms to determine flame spread rate over ethylene-tetrafluoroethylene wire insulation: Discussion on dilution gas effect based on temperature measurements, Proc. Combust. Inst. 28 (2000) 2905–2911.

[6] A.C. Fernandez-Pello, T. Hirano, Controlling Mechanisms of Flame Spread, Fire Sci. Technol. 2 (1982) 17–54.

[7] I.S. Wichman, Theory of opposed-flow flame spread, Prog. Energy Combust. Sci. 18 (1992) 553–593.

[8] C.K. Law, G.M. Faeth, Opportunities and challenges of combustion in microgravity, Prog. Energy Combust. Sci. 20 (1994) 65–113.

[9] P.D. Ronney, Understanding combustion processes through microgravity research, Symp. Combust. 27 (1998) 2485–2506.

[10] O. Fujita, Solid combustion research in microgravity as a basis of fire safety in space, Proc. Combust. Inst. 35 (2015) 2487–2502.

[11] X. Huang, J. Gao, A review of near-limit opposed fire spread, Fire Saf. J. 120 (2021) 103141.

[12] J.S. T'ien, Diffusion flame extinction at small stretch rates: The mechanism of radiative loss, Combust. Flame. 65 (1986) 31–34.

[13] S. Bhattacharjee, R.A. Altenkirch, The effect of surface radiation on flame spread in a quiescent, microgravity environment, Combust. Flame. 84 (1991) 160–169.

[14] T.-K. Oh, J.S. Lee, S.H. Chung, Effect of gas-phase and surface radiation on the structure and extinction of diffusion flames stabilized on a condensed fuel, Int. J. Heat Mass Transf. 37 (1994) 2893–2900.

[15] S. Takahashi, M. Kondou, K. Wakai, S. Bhattacharjee, Effect of radiation loss on flame spread over a thin PMMA sheet in microgravity, Proc. Combust. Inst. 29 (2002) 2579–2586.

[16] S. Bhattacharjee, R. Ayala, K. Wakai, S. Takahashi, Opposed-flow flame spread in microgravity-theoretical prediction of spread rate and flammability map, Proc. Combust. Inst. 30 (2005) 2279–2286.

[17] S. Bhattacharjee, K. Wakai, S. Takahashi, Predictions of a critical fuel thickness for flame extinction in a quiescent microgravity environment, Combust. Flame. 132 (2003) 523–532.

[18] S. Takahashi, T. Ebisawa, S. Bhattacharjee, T. Ihara, Simplified model for predicting difference between flammability limits of a thin material in normal gravity and microgravity environments, Proc. Combust. Inst. 35 (2015) 2535–2543.

[19] T. Delzeit, L. Carmignani, T. Matsuoka, S. Bhattacharjee, Influence of edge propagation on downward flame spread over three-dimensional PMMA samples, Proc. Combust. Inst. 37 (2019) 3203–3209.

[20] M.A. Delichatsios, Creeping flame spread: Energy balance and application to practical materials, Symp. Combust. 26 (1996) 1495–1503.

[21] M.A. Delichatsios, Relation of opposed flow (creeping) flame spread with extinction/ignition, Combust. Flame. 135 (2003) 441–447.

[22] S. Bhattacharjee, R. Nagarkar, Y. Nakamura, A correlation for an effective flow velocity for capturing the boundary layer effect in opposed-flow flame spread over thin fuels, Combust. Sci. Technol. 186 (2014) 975–987.

[23] S. Bhattacharjee, W. Tran, M. Laue, C. Paolini, Y. Nakamura, Experimental validation of a correlation capturing the boundary layer effect on spread rate in the kinetic regime of opposed-flow flame spread, Proc. Combust. Inst. 35 (2015) 2631–2638.

[24] K. Pohlhausen, Zur näherungsweisen Integration der Differentialgleichung der Iaminaren Grenzschicht, ZAMM - J. Appl. Math. Mech. / Zeitschrift Für Angew. Math. Und Mech. 1 (1921) 252–290.

[25] L. Carmignani, S. Bhattacharjee, S.L. Olson, P. V. Ferkul, Boundary Layer Effect on Opposed-Flow Flame Spread and Flame Length over Thin Polymethyl-Methacrylate in Microgravity, Combust. Sci.

Technol. 190 (2018) 534–548.
[26] L. Carmignani, G. Celniker, S. Bhattacharjee, The Effect of Boundary Layer on Blow-Off Extinction in Opposed-Flow Flame Spread over Thin Cellulose: Experiments and a Simplified Analysis, Fire Technol. 53 (2017) 967–982.
[27] Y. Nakamura, Y. Etoh, H. Yamashita, Effects of Velocity Boundary Layer on Opposed Flame Spread over a Thermally Thin Solid Fuel in Microgravity, Trans. Japan Soc. Mech. Eng. Ser. B. 69 (2003) 193–199.
[28] Z. Chen, Y. Ju, Theoretical analysis of the evolution from ignition kernel to flame ball and planar flame, Combust. Theory Model. 11 (2007) 427–453.
[29] Z. Chen, X. Gou, Y. Ju, Studies on the Outwardly and Inwardly Propagating Spherical Flames with Radiative Loss, Combust. Sci. Technol. 182 (2010) 124–142.
[30] H. Zhang, P. Guo, Z. Chen, Outwardly Propagating Spherical Flames with Thermally Sensitive Intermediate Kinetics and Radiative Loss, Combust. Sci. Technol. 185 (2013) 226–248.
[31] Z. Chen, Effects of radiative loss on premixed planar flame propagation, Proc. Combust. Inst. 38 (2021) 4683–4690.
[32] Y. Ju, H. Guo, K. Maruta, F. Liu, On the extinction limit and flammability limit of non-adiabatic stretched methane–air premixed flames, J. Fluid Mech. 342 (1997) 315–334.
[33] K. Maruta, M. Yoshida, H. Guo, Y. Ju, T. Niioka, Extinction of low-stretched diffusion flame in microgravity, Combust. Flame. 112 (1998) 181–187.
[34] S. Gordon, B.J. McBride, Computer Program for Calculation of Complex Chemical Equilibrium, NASA Ref. Publ. 1311. (1994) 1–2.
[35] S.H. Strogatz, Nonlinear Dynamics and Chaos: With Applications to Physics, Biology, Chemistry, and Engineering, 2nd ed., Westview Press, 2014.